

## METROLOGICAL ASPECTS OF SURFACE TOPOGRAPHIES PRODUCED BY DIFFERENT MACHINING OPERATIONS REGARDING THEIR POTENTIAL FUNCTIONALITY

Krzysztof Żak, Wit Grzesik

Opole University of Technology, Faculty of Mechanical Engineering, Mikolajczyka 5, 45-271 Opole, Poland  
(✉ k.zak@po.opole.pl, +48 77 449 8462, w.grzesik@po.opole.pl)

### Abstract

This paper presents a comprehensive methodology for measuring and characterizing the surface topographies on machined steel parts produced by precision machining operations. The performed case studies concern a wide spectrum of topographic features of surfaces with different geometrical structures but the same values of the arithmetic mean height  $S_a$ . The tested machining operations included hard turning operations performed with CBN tools, grinding operations with  $Al_2O_3$  ceramic and CBN wheels and superfinish using ceramic stones. As a result, several characteristic surface textures with the  $S_a$  roughness parameter value of about  $0.2 \mu m$  were thoroughly characterized and compared regarding their potential functional capabilities. Apart from the standard 2D and 3D roughness parameters, the fractal, motif and frequency parameters were taken in the consideration.

Keywords: surface metrology, surface topography, surface roughness, areal parameters, machining operations.

© 2017 Polish Academy of Sciences. All rights reserved

### 1. Introduction

The visible progress in surface metrology enables the surface features generated by modern manufacturing processes to be characterized with a higher accuracy using, apart from standardized 2D roughness parameters, a number of the areal field (3D) parameters. In general, they are defined as sets of S-parameters and V-parameters [1, 2]. This metrological challenge concerns a big group of machine parts with an increased hardness of 45–60 HRC produced by precision ( $R_z = 2.5\text{--}4 \mu m$ ) and high-precision ( $R_z < 1 \mu m$ ) machining operations using superhard (mainly PCBN) cutting tools. These advanced machining processes have been an alternative to grinding for three decades [3, 4] due to their high flexibility, possible complete machining, smaller ecological impact and higher *material removal rate* (MRR) [5, 6]. However, grinding offers essential advantages in higher part dimensional accuracy and achievable higher productivity in comparison with alternative machining processes. Conventional grinding using ceramic wheels is unable to meet the production requirements concerning hardened steels. Thus, grinding with super abrasive (CBN and PCD) wheels becomes the optimum solution, especially in automotive industry.

The discussion platform concerning the economically and technologically motivated replacement of grinding by cutting with superhard cutting tools also focuses on the capabilities of produced profiles against the functionality of the machined surfaces [7]. This is because cutting and abrasive processes generate different surface structures which influence distinctly their functional properties such as resistance to abrasive wear, fluid retention ability and fatigue and contact strength [8]. Earlier concepts presented in [7] include only 2D height and amplitude parameters and the *bearing area curves* (BACs). Moreover, it has been observed that produced surface topographies are not geometrically similar, although the  $R_a$  or  $R_z$  roughness parameters

are nearly of the same values. This implies the necessity of performing more extended and advanced measurements.

The first characterization and comparison of surface textures produced by turning and grinding operations on hardened steel parts using a set of 3D roughness parameters is presented in [9]. The 2D and 3D comparison, more oriented towards bearing area parameters, related to precision cutting and abrasive operations, is provided in [10]. The objective of this study is a comprehensive characterization and comparison of the surface textures of representative hard turned, and differently ground and honed surfaces using a number of standardized 3D roughness parameters as well as the fractal dimension, motif and frequency parameters. This wide spectrum of measurement techniques seems to be adequate for the description of complex textures produced by random machining processes.

## 2. Machining tests and measurements of surface roughness

Cylindrical samples made of a 41Cr4 hardened ( $57 \pm 1$  HRC) steel with an initial roughness average value of  $Sa = 0.42 \mu\text{m}$  were differently finished by turning, grinding and superfinishing in order to reduce the Sa parameter value to about  $0.2 \mu\text{m}$ .

The machine tools were an Okuma Genos L200E-M CNC lathe and a conventional cylindrical grinding machine. The machining conditions are as follows:

1. *Hard turning* (HT) using a CBN TNGA 160408 S01030 chamfered insert,  $v_c = 150$  m/min,  $f = 0.06$  mm/rev,  $a_p = 0.15$  mm.
2. Cylindrical grinding using an electro-corundum ( $\text{Al}_2\text{O}_3$ ) (GR-CW), a  $350 \times 25 \times 127$  32A grinding wheel,  $v_c = 11.9$  m/s,  $a_e = 0.025$  mm,  $f_a = 3.5$  mm/rev.
3. Cylindrical grinding using an INTER DIAMENT B107 K100 SV grinding wheel (GR-CBNW),  $v_c = 36$  m/s,  $a_e = 0.025$  mm,  $f_a = 1.6$  mm/rev.
4. External honing (*super-finish*) SF using a 99A320N10V ceramic stone, an oscillation frequency of 680 osc/min and an amplitude of 3.5 mm, an applied force of 40 N, a cooling and lubrication medium – 85% kerosene and 15% machine oil.

Surface topographies generated by selected machining operations were recorded using a 3D contact profilometer with a diamond stylus radius of  $2 \pm 0.5 \mu\text{m}$ . The scanning process was performed on small,  $250 \mu\text{m} \times 250 \mu\text{m}$  square shape surfaces in order to generate 201 different surface profiles by the diamond stylus. The measurement resolution along X and Z axes obtained with an inductive transducer for roughness measurements is equal to  $0.001 \mu\text{m}$ . The measuring signals were filtered using a Gaussian digital filter. The raw data were automatically inserted into a Digital Surf, Mountains® Map package in order to determine both 2D and 3D roughness parameters and perform 3D visualization of the machined surfaces. In consequence, the representative values of surface roughness were determined as the average values from each of 201 sets of measurements performed on individual profiles.

The obtained surface topographies were described based on the following four groups of parameters: a) standardized 2D and 3D surface roughness parameters: height, amplitude, horizontal, hybrid and functional defined in the ISO 25178 standard [2, 11]; b) fractal dimension; c) standardized motif parameters and d) frequency spectra characteristics.

## 3. Experimental results and discussion

### 3.1. Characterization of surface topographies

Representative surface topographies obtained in *hard turning* (HT) and abrasive (both GR and SF) operations are visualized in Figs. 1a to 1d. Regarding the surface quality criterion these

operations can be classified as precision machining, because the maximum roughness height  $Rz < 2 \mu\text{m}$  [10].

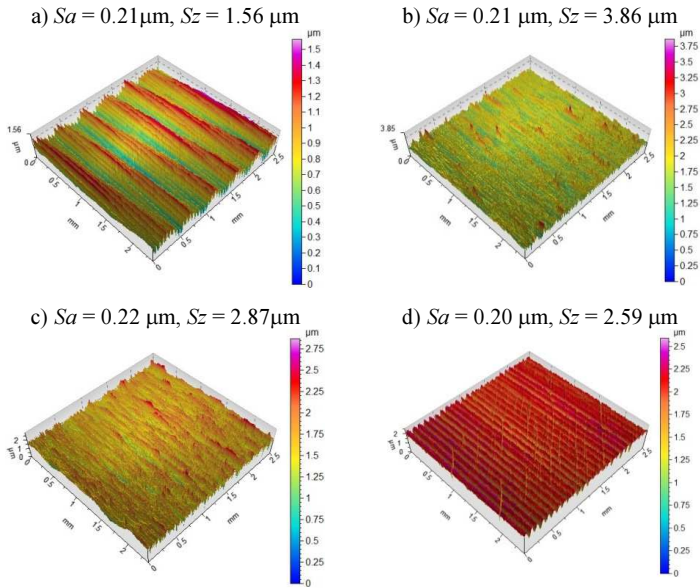


Fig. 1. Surface textures produced by HT (a); ground using  $\text{Al}_2\text{O}_3$  (b); CBN wheel (c) and honed (d).

The measured  $Sa$  values range between 0.20 and 0.22  $\mu\text{m}$ . As specified in Fig. 1,  $Sz$  parameter increases from 1.56  $\mu\text{m}$  for hard turning to 3.86  $\mu\text{m}$  for grinding with  $\text{Al}_2\text{O}_3$  wheel, which evidently suggests different surface functionality.

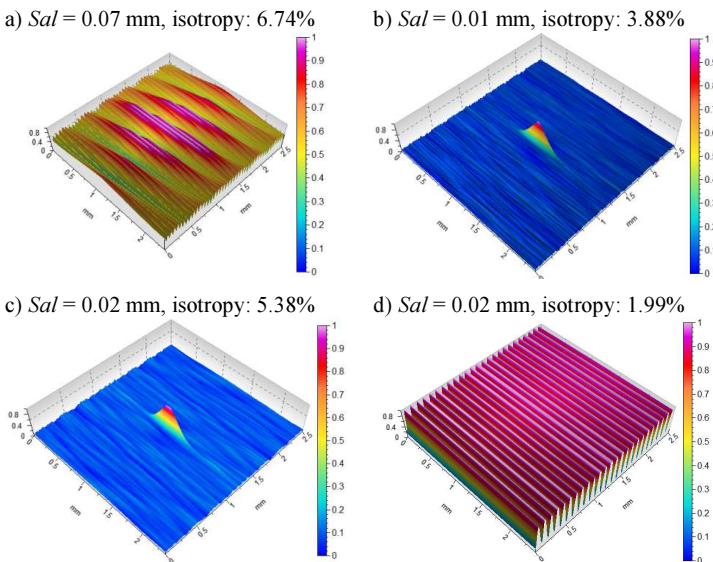


Fig. 2. Representative autocorrelation functions for turned (a); ground (b, c) and honed (d) surfaces.

The autocorrelation function (ACF) enables to distinguish the isotropic content from mixed isotropic-anisotropic surfaces which represent typical machined surfaces. As shown in Fig. 2, all machined surfaces have a strong anisotropy. This is because the autocorrelation has a central lobe which extends along one direction. The turned and honed surfaces are periodic-anisotropic (Figs. 2a and 2d) because they have other maxima which indicate the periodicity of these surfaces. The ground surfaces are mixed, between anisotropic and random structures (Figs. 2b and 2c) because the ACF represents one central lobe. The values of the fastest decay autocorrelation length ( $S_{al}$ ) are equal to 0.07 for hard turned and 0.01 or 0.02 for abrasive treated surfaces, respectively. A larger value of  $S_{al} = 0.07$  for the turned surface denotes that it is dominated by low spatial frequency components (see Fig. 12a). Dynamic influences of the machining system are reproduced along the lays and, as a result, the “central lobe” of the ACF decays faster in the direction parallel to the periodicity of the lay.

### 3.2. Characterization of function related parameters

Figure 3 presents shapes of 3D BACs and associated ADF curves obtained for the compared machining operations. In particular, hard turning (1) produces surfaces with a positive skew  $S_{sk} = 0.24$  but finish grinding (2 and 3) generates surfaces with a negative skew  $S_{sk} = -0.31$  for GR-CW versus  $-0.48$  for GR-CBNW. Moreover, Fig. 3b suggests that hard turning and grinding produced topographies with diametrically different ADF shapes which result in various bearing and contact properties. The superior bearing properties ( $S_{sk} = -0.69$ ) were obtained when sharp irregularities produced by hard turning were removed by abrasive stone during additional honing (BAC #4 in Fig. 3a). Additionally, values of the areal material ratio  $S_{mr}(c)$ , the inverse areal material ratio  $S_{dc}(mr)$  and the peak extreme height  $S_{xp}$  are given in Fig. 3a.

- a) 1.  $S_{dc} = 0.66 \mu\text{m}$ ,  $S_{xp} = 0.44 \mu\text{m}$ , 2.  $S_{dc} = 1.97 \mu\text{m}$ ,  $S_{xp} = 0.60 \mu\text{m}$ , 3.  $S_{dc} = 1.13 \mu\text{m}$ ,  $S_{xp} = 0.65 \mu\text{m}$ , 4.  $S_{dc} = 0.46 \mu\text{m}$ ,  $S_{xp} = 0.61 \mu\text{m}$   
 b) 1.  $S_{sk} = 0.24$ ,  $S_{ku} = 2.56$ , 2.  $S_{sk} = -0.31$ ,  $S_{ku} = 5.41$ , 3.  $S_{sk} = -0.48$ ,  $S_{ku} = 3.70$ , 4.  $S_{sk} = -0.69$ ,  $S_{ku} = 3.03$

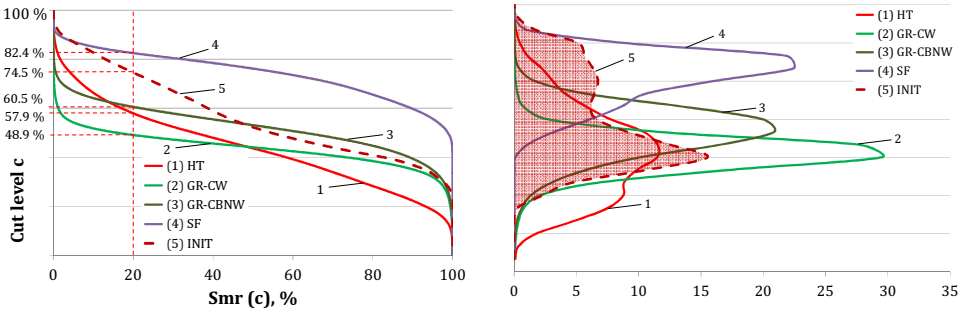


Fig. 3. 3D BAC shapes (a) and ADF distributions (b) for turned (1); ground (2 and 3) and honed (4) surfaces; the initial hard-turned surface (5).

Additional information on the fluid retention can be obtained using a technique of vectorisation of micro-valleys’ network (Fig. 4) available in the used Mountain Map package [12] generated on the machined surface. The maximum depth of valleys is between 1 and 2  $\mu\text{m}$  and their width is predominantly equal to 0.5  $\mu\text{m}$ . Additionally, the average density of valleys is between 500 and 700  $\text{cm}/\text{cm}^2$ , respectively. This comparison indicates that abrasive operations produce surfaces with a greater number of deeper valleys (Fig. 4b). These data coincide well with the distributions of the volume functional parameter ( $V_{mp}$  and  $V_{vv}$ ) shown in Fig. 5. The functional analysis of 3D BACs is based on four volume parameters, including:

the peak material volume ( $V_{mp}$ ), the core material volume ( $V_{mc}$ ), the core void volume ( $V_{vc}$ ) and the valley void volume ( $V_{vv}$ ) ones. [1, 2]. Their values obtained for HT and abrasive operations are as follows (in order HT/GR-CW/GR-CBNW/SF):  $V_{mp} = 0.0125/ 0.0150/ 0.0112/0.0063 \mu\text{m}^3/\mu\text{m}^2$ ;  $V_{mc} = 0.254/0.225/0.247/0.252 \mu\text{m}^3/\mu\text{m}^2$ ;  $V_{vc} = 0.342/0.292/ 0.310/0.255 \mu\text{m}^3/\mu\text{m}^2$ ;  $V_{vv} = 0.0213/0.0383/0.0403/0.0353 \mu\text{m}^3/\mu\text{m}^2$ . For instance, higher values of  $V_{vv} = 0.0383$  and  $0.0403 \mu\text{m}^3/\mu\text{m}^2$  suggest better fluid retention ability of ground surfaces (for a turned surface  $V_{vv} = 0.0213 \mu\text{m}^3/\mu\text{m}^2$ ).

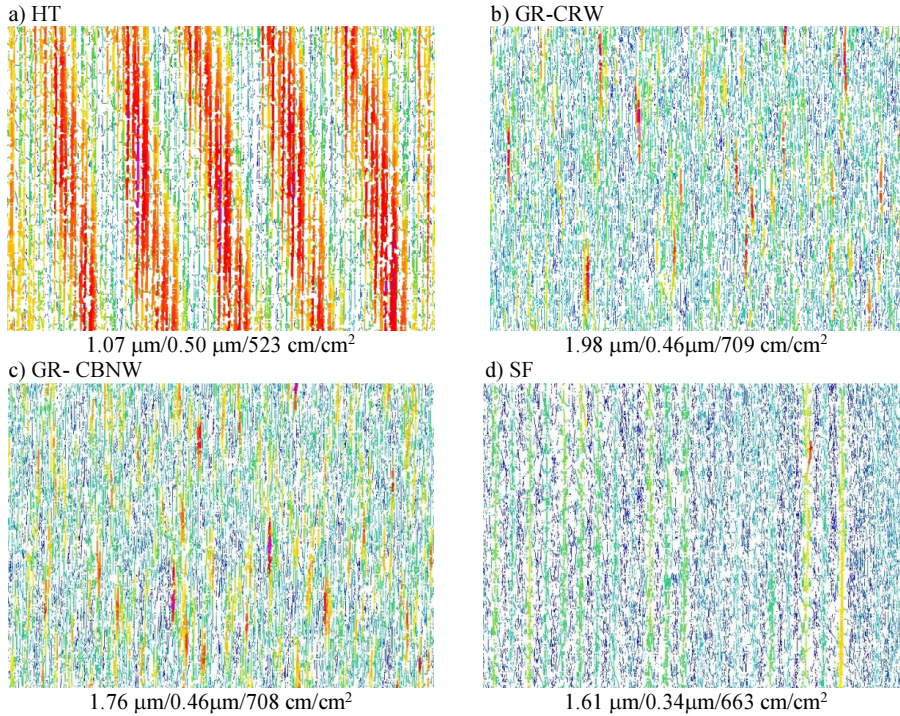


Fig. 4. Vectorised micro-valley networks for turned (a); ground with  $\text{Al}_2\text{O}_3$  wheel (b); ground with CBN wheel (c) and honed (d) surfaces. Three values give the average depth, width and density of micro-valleys.

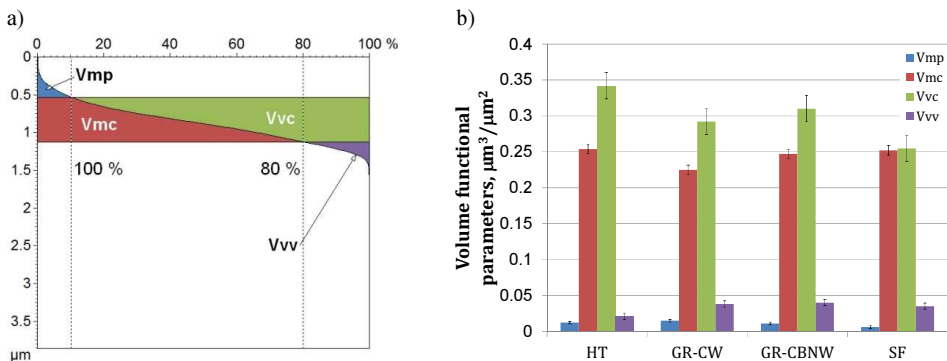


Fig. 5. Functional volumetric parameters for different finishing operations: distribution of volume parameters for hard turning (a); distributions for all machining operations (b).

The comparison of function-related parameters [2] is given in Figs. 6 and 7. In these case studies three areal ( $V$ ) material ratio parameters – the reduced core ( $Sk$ ), peak ( $Spk$ ) and valley ( $Svk$ ) height (Fig. 6) and their ratios –  $Spk/Sk$ ,  $Svk/Sk$ ,  $Spk/Svk$  (Fig. 7) were used in order to assess the nature of specific surface textures. In particular, the ratio of  $Spk/Sk$  may be helpful to distinguish between two surfaces with indistinguishable roughness average  $Sa$  [11].

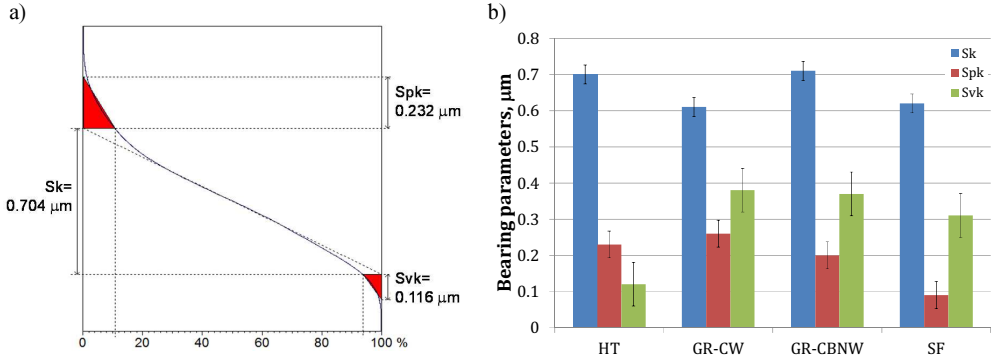


Fig. 6. Areal bearing area parameters for different finishing operations: distribution for hard turning (a); distributions for all machining processes (b).

It can be seen in Fig. 6b that all cutting and abrasive operations generated surfaces with comparable values of the reduced core height between 0.6–0.7 μm. On the other hand, visible differences between the reduced peak ( $Spk$ ) height and reduced valley ( $Svk$ ) height can be observed in Fig. 6b.

Moreover, both ground surfaces with the same  $Sa$  have vastly different  $Spk/Sk$  values of 0.426 and 0.282 (Fig. 7a). They are further reduced to 0.145 by honing. As shown in Fig. 7b, the ratio of  $Spk/Sk$  correlates well also with the  $Vmp$  volume parameter, whereas the ratio of  $Svk/Sk$  with the  $Vvc$  volume parameter and micro-valleys density. Additional relationships can be observed (Fig. 7a) between the ratio of  $Spk/Svk$  and  $Sdc$  and  $Sxp$  material ratio parameters.

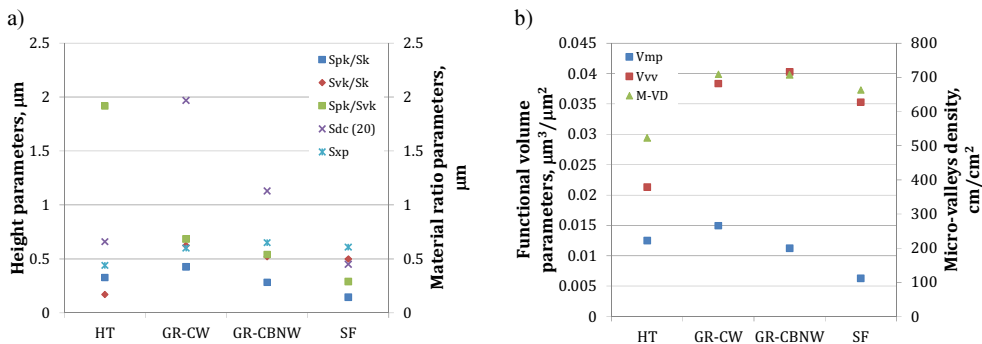


Fig. 7. Functional relationships between selected 3D V-parameters.

### 3.3. Characterization of spatial and hybrid parameters

The set of 3D parameters includes four spatial parameters, three of which are texture parameters. The ground and – especially – honed surfaces contain distinctly more summits within the scanned area –  $Sds = 2006.1$  1/mm<sup>2</sup> (SF) versus 1440.7 1/mm<sup>2</sup> (HT). The comparable

small texture aspect ratio  $Str = 0.02\text{--}0.07$  for all machined surfaces indicates stronger directionality (anisotropy) but its values for both cutting and abrasive operations, which are less than 0.1, are characteristic for highly anisotropic surfaces [13]. The texture direction  $Std$  close to  $90^\circ$  for all three surfaces indicates that the dominant surface lay is perpendicular to the measurement direction. The values of  $Sal$  parameter are given in Fig. 2.

The values of three 3D hybrid parameters emphasize additional geometrical differences in the compared textures. Higher slopes  $Sdq$  of about  $6^\circ$  were obtained for ground surfaces versus  $3^\circ$  for turned and honed surfaces. The values of average summit curvature  $Ssc$  of about  $0.007\ \mu\text{m}^{-1}$  for the turned and honed surface and about  $0.02\ \mu\text{m}^{-1}$  for the ground surfaces are typical for machined surfaces ( $0.004\text{--}0.03\ \mu\text{m}^{-1}$  given in [13]). The  $Sdr$  parameter (the developed interfacial area ratio) of 0.16% is higher for the ground surfaces (Fig. 1b and c) than for the turned and honed surface (Figs. 1a and 1 d) – 0.04%/0.03%.

### 3.4. Motifs and fractals

The motif analysis is performed on an unfiltered surface profile divided into a series of windows [13, 14], as shown for all machining variants in Fig. 8. In this study the mean depth of roughness motif  $R$ , the mean spacing of roughness motif  $AR$  and the largest motif height  $Rx$  were analysed.

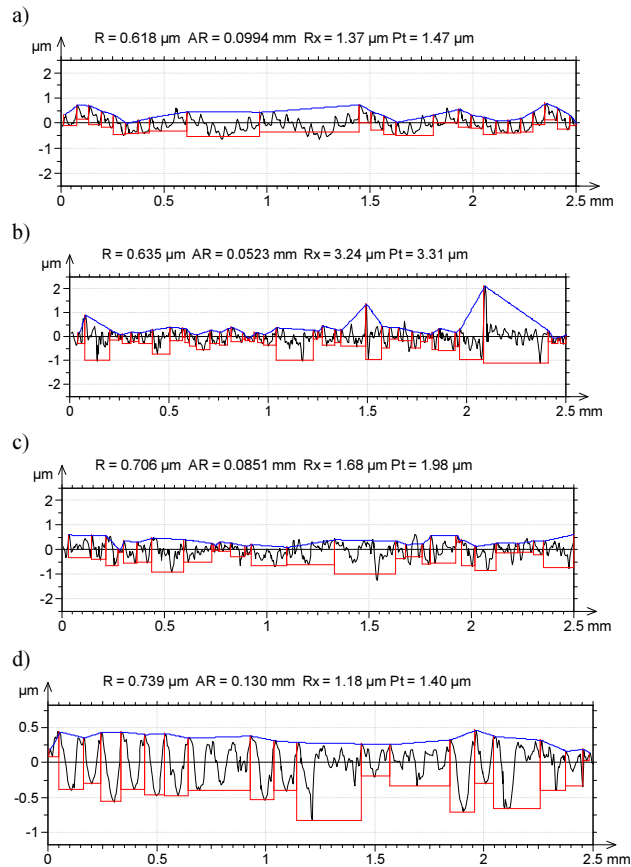


Fig. 8. Examples of the motif graphs for hard turned (a); ground with  $\text{Al}_2\text{O}_3$  wheel (b); ground with CBN wheel (c) and honed (d) surfaces.

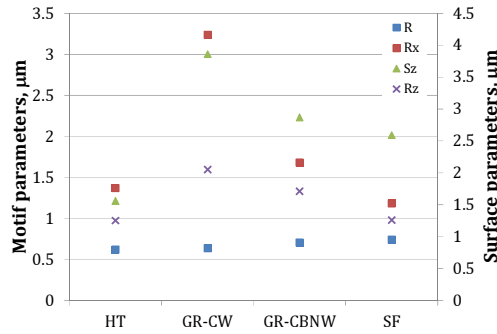
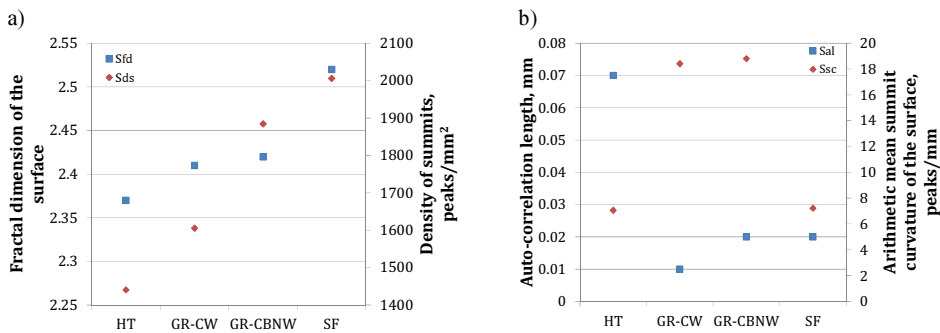


Fig. 9. Functional relationships between  $Sz(Rz)$  and  $Rx(R)$  motif parameters.

The ground surfaces include distinctly deeper pits ( $Rx = 1.68$  and  $2.55 \mu\text{m}$ ) in comparison with the hard-turned and honed surfaces ( $Rx = 1.37/1.18 \mu\text{m}$ ), which is in accordance with the volume bearing parameters (Fig. 5). Fig. 9 shows that the  $Rx$  motif parameter is stronger correlated with the  $Sz$  parameter than with the  $Rz$  one, although motifs are based on the 2D analysis. On the other hand, the  $R$  motif parameter of  $0.6\text{--}0.7 \mu\text{m}$  seems to be independent of the used machining operations and coincides with the  $Rz$  changes.



*Sfd*: HT-2.37, GR-CW-2.41, GR-CBNW-2.42, SF-2.52;

*Sds*: HT-1441 1/mm<sup>2</sup>, GR-CW-1605 1/mm<sup>2</sup>, GR-CBNW- 1885 1/mm<sup>2</sup>, SF-2006 1/mm<sup>2</sup>.

Fig. 10. Functional relationships between selected 3D S-parameters and the fractal dimension.

The fractal dimension concept enables a description of the complexity of engineering surfaces in the form of a single number. The fractal dimension may vary between the theoretical limits of 1 for a straight line and 2 for a space-filling curve. It should be noted that real machined surfaces are called multifractal because obviously they are formed by several different processes, each with its characteristic topographical features [14]. Digital Surf, Mountains® Map software [15] enables to calculate the fractal dimension for a surface profile or real surface by means of a method of enclosing boxes or morphological envelopes. In the method of enclosing boxes in real units, applied in this study, the fractal dimension is determined by calculating the slope of regression line which corresponds best to the  $\ln N$  versus  $\ln \epsilon$  plot (where  $N$  is the number of boxes and  $\epsilon$  is the size of a box).

The values of 3D fractal dimension  $Sfd$  determined by means of the method of enclosing boxes are equal to 2.37, 2.41/2.42 and 2.52 for turned, ground and honed surfaces. On the other hand, the values of 2D fractal dimension  $D$  determined from the surface profiles are equal to 1.08, 1.56/1.61 and 1.66, respectively.

The functional relationships between fractal dimension  $Sfd$  and  $Sal$ ,  $Ssc$  and  $Sds$  spatial and hybrid parameters are revealed in Fig. 10. It can be noticed in Fig. 10a that the  $Sfd$  is strongly correlated with the density of summits ( $Sds$ ) and  $Sfd = 2.52$  corresponds with the maximum value of  $Sds = 2006 \text{ 1/mm}^2$  determined for the honed surface. For this function ( $Sfd = 5 \times 10 - 7Sds - 0.0015(Sds)^2 + 3.4693$ ) the  $R$ -square is equal to 0.8363. In addition, it correlates with the arithmetic summit curvature ( $Ssc$ ) and the autocorrelation length  $Sal$  parameter which characterize the texture anisotropy (Figs. 2 and 10b).

### 3.5. Frequency analysis

The characteristic PSD spectra obtained for hard turned, ground and honed surfaces are presented in Fig. 11. The PSD is very sensitive to all disturbances of the generated surfaces appearing in the machining system.

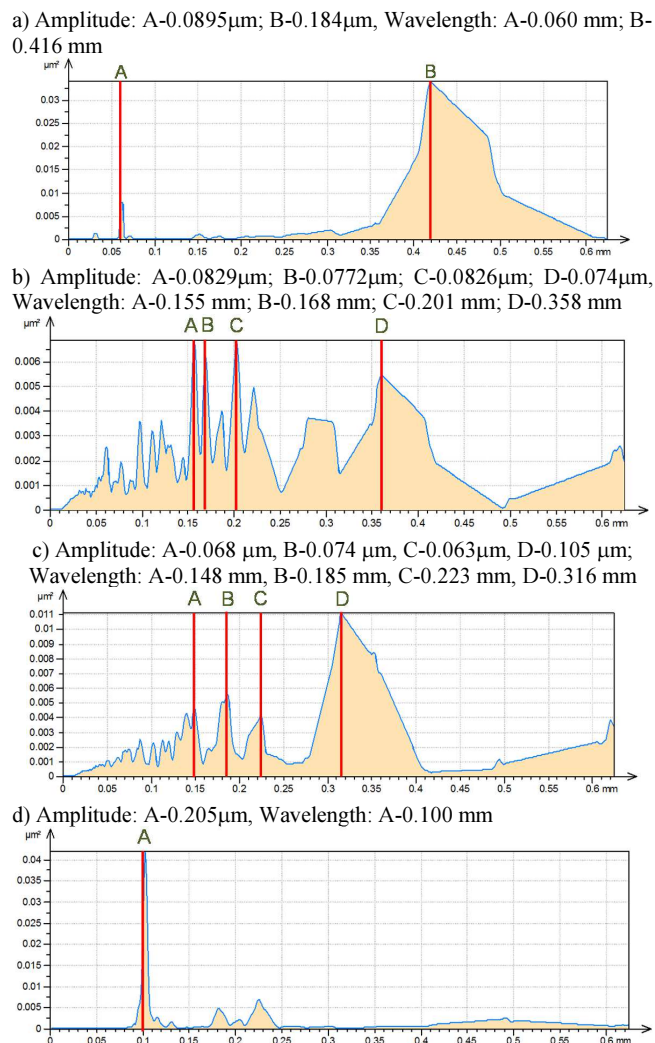


Fig. 11. The averaged power spectral density for turned (a); ground with  $\text{Al}_2\text{O}_3$  wheel (b); ground with CBN wheel (c) and honed (d) surfaces.

It is evident from Fig. 11a that the PSD spectrum contains only one low-frequency component with the same wavelength as the feed rate of 0.06 mm (60  $\mu\text{m}$ ) and the amplitude of 0.09  $\mu\text{m}$ . On the other hand (Figs. 11b and 11c), the ground surfaces contain several components with longer wavelengths but distinctly lower amplitudes of 0.04–0.07  $\mu\text{m}$  than the hard-turned surfaces. In particular, very small amplitudes of about 0.07  $\mu\text{m}$  were recorded for the surfaces produced by grinding using a CBN wheel (Fig. 11c). On the other hand, the highest amplitude of about 0.2  $\mu\text{m}$  appeared during the honing operation which was performed on a conventional lathe.

#### 4. Conclusions

1. Distinct changes of topographical features of machined surfaces produced by different cutting and abrasive processes are revealed using both standardized and non-standardized measuring techniques. According to the engineering knowledge this enables to generate surfaces with desired functional properties, for instance with required bearing or locking properties, resistance to abrasive wear, fluid retention capability, fatigue and contact strength, depending on their engineering applications.
2. Precision grinding and super-finish operations cause that successively more material is concentrated in the vicinity of surface peaks. For these cases the ADF function has a symmetrical shape with a large kurtosis and/or a large skew.
3. Comparing surface topographies using the autocorrelation operator indicates their strong anisotropy and the necessity of 3D measurement.
4. 3D bearing area curves and appropriate functional parameters suggest, according to [13], that the ground hard surfaces have enhanced fluid retention abilities. This is due to a large negative  $Ssk$  value and higher  $V_{VV}$  volumes for ground textures.
5. The hard turned and CBN-ground textures have comparable  $V_{mp}$  and  $Spk$  parameter values and similar tribological properties. According to the engineering practice demonstrated in [12] and [13] the best tribological performance of the honed surface is due to minimum  $V_{mp}$  and  $Spk$  values.
6. The fractal dimension  $Sdf$  correlates well with the density of summits. Because a higher value of the  $Sdf$  parameter denotes a large surface area (a larger  $Sdr$  parameter), a possible consequence should be that in such a case the normal contact pressure decreases and the wear rate decreases with increasing the  $Sdf$  value.
7. The  $PSD$  charts enable directly to recognize a possible influence of the machining system stability on the surface texture and, as a result, also to eliminate inconvenient machining conditions causing excessive vibrations.

#### List of abbreviations

GR – grinding  
HT – hard turning  
SF – super finishing  
S-parameters – Surface-parameters  
V-parameters – Volume-parameters  
ACF – autocorrelation function  
ADF – amplitude density function  
BAC – bearing area (material ratio) curve  
CBN – cubic boron nitride  
MRR – machining removal rate

PCD – polycrystalline diamond

PSD – power spectral density

AACF – autocorrelation function

GR-CW – grinding (GR) using conventional wheel (CW)

GR-CBNW – grinding (GR) using CBN wheel (CBNW)

HT/GR-CW – hard turning/grinding using conventional wheel sequential process

HT/ GR-CBNW – hard turning/ grinding using CBN wheel sequential process

## References

- [1] Jiang, X.Jm, Whitehouse, D.J. (2012). Technological shifts in surface metrology. *CIRP Annals-Manuf. Technol.*, 61(2), 815–836.
- [2] Leach, R. (ed.) (2013). *Characterization of areal surface texture*. Berlin, Springer-Verlag.
- [3] Grzesik, W. (2008). *Advanced machining processes of metallic materials*. Elsevier, Amsterdam.
- [4] Klocke, F. (2011). *Manufacturing processes 1. Cutting*, Berlin, Springer.
- [5] König, W., Berkold, A., Koch, K.F. (1993). Turning versus grinding- a comparison of surface integrity aspects and attainable accuracies. *CIRP Annals-Manuf. Technol.*, 42(1), 39–43.
- [6] Davim, J.P. (ed.) (2011). *Machining of hard materials*. London, Springer.
- [7] Klocke, F., Brinksmeier, E., Weinert, K. (2005). Capability profile of hard cutting and grinding processes. *CIRP Annals-Manuf. Technol.*, 54(2), 557–580.
- [8] Grzesik, W., (2016). Prediction of the functional performance of machined components based on surface topography: a survey. *J. Mater. Eng. Perf.*, 25(10), 4460–4468.
- [9] Waikar, R.A., Guo, Y.B. (2008). A comprehensive characterization of 3D surface topography induced by hard turning versus grinding. *J. Mat. Proc. Technol.*, 197, 189–199.
- [10] Grzesik, W., Rech, J., Wanat, T. (2007). Surface finish on hardened bearing steel parts produced by superhard and abrasive tools. *Int. J. Mach. Tools and Manuf.*, 47, 255–262.
- [11] ISO 25178, part 2 (2012), *Geometrical product specification (GPS)– surface texture: areal. Terms, definitions and surface texture parameters*, ISO.
- [12] Digital Surf, Mountains® Map software, [www.digitalsurf.com](http://www.digitalsurf.com).
- [13] Griffiths, B. (2001). *Manufacturing surface technology. Surface integrity and functional performance*. London, Penton Press.
- [14] Dietzsch, M., Papenfuss, K., Hartman, T. (1998). The MOTIF-method (ISO 12085)- a suitable description for functional, manufactural and metrological requirements. *Int. J. Mach. Tools and Manuf.*, 38, 625–632.
- [15] Thomas, T.R., (1999). *Rough Surfaces*. London, Imperial College Press.